Carrier-Transport-Limited Modulation Bandwidth in Distributed Reflector Lasers With Wirelike Active Regions

Daisuke Takahashi, *Member, IEEE*, SeungHun Lee, *Member, IEEE*, Mizuki Shirao, *Member, IEEE*, Takahiko Shindo, *Student Member, IEEE*, Keisuke Shinno, Tomohiro Amemiya, *Member, IEEE*, Nobuhiko Nishiyama, *Senior Member, IEEE*, and Shigehisa Arai, *Fellow, IEEE*

***Abstract*— High-speed direct modulation capability was investigated in 1.55-μm GaInAsP/InP distributed reflector (DR) lasers with wirelike active regions in terms of carrier transport from GaInAsP optical confinement layers (OCLs) to the active regions. Theoretical analysis revealed strong dependence of the modulation bandwidth on the thickness of the OCLs and width of the wirelike active regions. To confirm this prediction, two DR lasers with OCLs of different thicknesses (120 and 40 nm) were fabricated and their 3-dB bandwidths ($f_{3\ dB}$) under small-signal modulation were compared. The device with the narrower OCL exhibited $f_{3\ dB}$ exceeding 15 GHz and clear eye opening under 25 Gb/s modulation, whereas that with the thicker OCL had $f_{3\ dB}$ of only 2 GHz. These results were in good agreement with the theoretical predictions.**

***Index Terms*— Distributed reflector (DR) laser, high-speed modulation, low power consumption, semiconductor laser.**

I. Introduction

THE rapid increase in data traffic due to the emergence of innovative services delivered through broadband Internet demands access networks with higher bit rates. Therefore, high-speed communication technologies such as 40 and 100 GbE are being standardized and developed. For the long-wavelength range, wavelength division multiplexing of four wavelengths times 25 and 10 Gbps is used in 100 and 40 GbE, respectively.

Thus, research efforts to realize such high speeds with inexpensive modules have mainly focused on distributed feedback (DFB) lasers integrated with an electroabsorption modulator [1–3] (EML) and direct modulation lasers [4–7] (DMLs) designed for high modulation efficiencies. Although EMLs are used in first-generation 100 GbE modules owing to their speed capability and relatively low chirping, DMLs could have advantages such as low power consumption and cost-effectiveness for future-generation modules. DFB lasers integrated with a passive feedback section [8, 9] and distributed Bragg reflector (DBR) lasers having a short gain section [10] have also been studied. A stable single-mode operation and good dynamic properties of DFB lasers with etched quantum-wells structure were demonstrated [11, 12], and a sub-mA threshold current operation as well as a stable single-mode operation was demonstrated for DFB lasers with vertically etched wirelike active regions [13].

A distributed reflector (DR) laser, consisting of DFB and DBR sections, is a good candidate design for a DML in such applications since stable single-mode operation with high output efficiency from one side facet can be attained and superior lasing properties such as modulation sensitivity and spectral chirping have been theoretically predicted [14]. Recently, DR lasers with GaInAsP multiple-quantum-well wirelike active regions, as shown in Fig. 1, have been demonstrated with a low threshold current of around 1 mA, high differential quantum efficiency of around 50%/facet, and a stable single-mode property with a sub-mode suppression ratio (SMSR) exceeding 40 dB because of the small volume of the active region and a strong index-coupling grating structure [15–17]. However, their 3 dB bandwidth under direct modulation was measured to be less than 10 GHz even though data transmission of 5 Gbps-10 km and 10 Gbps-10 km were achieved [18].

In this paper, we discuss the theoretical modulation bandwidth of DR lasers with wirelike active regions limited by carrier transport from GaInAsP optical confinement layers (OCLs) to wirelike active regions and then compare with experimental results for two types of DR lasers with different OCL thicknesses. As a result, the 3 dB bandwidth of the DR laser with the thin (40 nm) OCL was 15 GHz, which was much greater than that obtained with a thicker (120 nm) OCL, and high-speed operation was demonstrated with relatively low power consumption. In section 2, the 3 dB bandwidth dependence on the thickness of the OCL is given with a parameter of the width of wirelike active regions. Section 3 explains

Manuscript received September 20, 2011; revised December 22, 2011; accepted March 8, 2012. Date of publication March 13, 2012; date of current version April 20, 2012. This work was supported in part by the Japan Society for Promotion of Science (JSPS) and the Ministry of Education, Culture, Sports, Science and Technology (MEXT), Grants-in-Aid for Scientific Research under Grant 19002009, Grant 22360138, Grant 21226010, Grant 21860031, Grant 09J08757, and Grant 10J08973.

D. Takahashi, S. Lee, M. Shirao, T. Shindo, K. Shinno, and N. Nishiyama are with the Department of Electrical and Electronic Engineering, Tokyo Institute of Technology, Tokyo 152-8552, Japan (e-mail: takahashi.12.12@gmail.com; huni@quantum.pe.titech.ac.jp; shirao.m.aa@m.titech.ac.jp; shindou.t.aa@m.titech.ac.jp; shinno.k.aa@m.titech.ac.jp; n-nishi@pe.titech.ac.jp).

T. Amemiya and S. Arai are with the Department of Electrical and Electronic Engineering, Tokyo Institute of Technology, Tokyo 152-8552, Japan, and also with the Quantum Nanoelectronics Research Center, Tokyo Institute of Technology, Tokyo 152-8552, Japan (e-mail: amemiya.t.ab@m.titech.ac.jp; arai@pe.titech.ac.jp).

Color versions of one or more of the figures in this paper are available online at http://ieeexplore.ieee.org.

Digital Object Identifier 10.1109/JQE.2012.2190822

0018–9197/$31.00 © 2012 IEEE

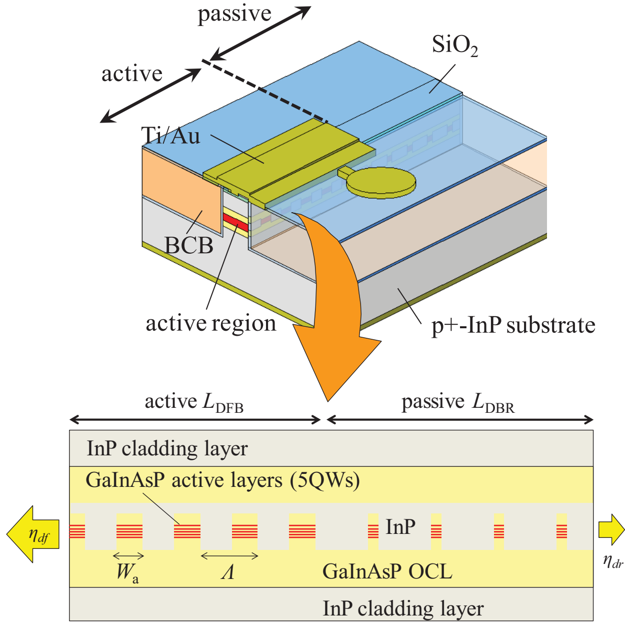

Fig. 1. Schematic and cross-sectional structures of DR laser with wirelike active regions.

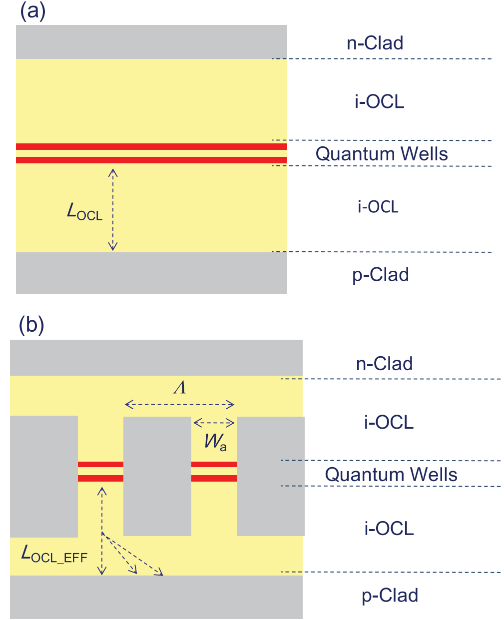

Fig. 2. Cross-sectional structures of (a) SCH QW active region and (b) SCH with wirelike active regions.

the device structure and fabrication processes of DR lasers used for measurements of direct modulation characteristics. In section 4, fundamental light output properties and modulation characteristics, such as the bias current dependence of the relaxation oscillation frequency and small signal response of two types of DR lasers are given and discussed. Large-signal modulation experiments at 10 and 25 Gbps are also presented.

II. Model and Theoretical Analyses of 3-dB Bandwidth

Figure 2 is a cross sectional schematic diagram of (a) the separate–confinement heterostructure (SCH) consisting of a quantum-well (QW) active region sandwiched by OCLs and (b) a SCH with wirelike active regions. It is known that carrier transport in the OCLs restricts the modulation bandwidth and this is mainly governed by the classical current continuity equations that describe the diffusion, recombination, and drift of carriers across the SCH in the presence of an electric field. The transport time $\tau_{\rm OCL}$ and 3dB cut-off frequency $f_{\rm 3dB_OCL}$ due to the carrier transport in the OCLs obtained from the current continuity equations [19, 20] are

$$\tau_{OCL} = \frac{L_{OCL}^2}{2D_a},$$
$$f_{3dB_OCL} = \frac{1}{2\pi\,\tau_{OCL}}\frac{2}{2\pi\,L_{OCL}^2} \quad (1)$$

where $L_{\rm OCL}$ is the thickness of the GaInAsP OCL and $D_a = 2D_nD_h/(D_n + D_h)$ is an ambipolar diffusion coefficient (D_n and D_h are the diffusion coefficients of electrons and holes, respectively). It is known that the 3dB frequency is inversely proportional to the square of $L_{\rm OCL}$; hence, it is sensitive to the thickness of the OCL.

Figure 2(b) shows that carriers in the OCL below the groove embedded with InP are transported a distance longer than $L_{\rm OCL}$; hence, an effective length $L_{\rm OCL_EFF}$ should be considered for DFB or DR lasers consisting of wirelike active regions. In this work, we estimated the carrier-transport portion of the modulation bandwidth (3 dB frequency $f_{\rm 3dB_OCL}$) of wirelike active regions by numerical calculation using the two-dimensional diffusion equation and discretized it employing forward-time centered space. The two-dimensional diffusion equation is expressed as

$$\frac{\partial T(x,y,t)}{\partial t} = D_h\frac{\partial^2 T(x,y,t)}{\partial x^2} + D_h\frac{\partial^2 T(x,y,t)}{\partial y^2} \quad (2)$$

where $T(x,y,t)$ is the carrier density at position (x, y) and time t. We calculated the diffusion of holes because the limitation of diffusion is dominated by the holes owing to their mobility being lower than that of electrons. Through discretization, the equation can be modified as

$$\begin{aligned} T(x_j, y_k, t_{n+1}) = T(x_j, y_k, t_n) &+ \frac{D_a\tau}{h_x^2}\{T(x_j+h, y_k, t_n) \\ &+T(x_j-h, y_k, t_n) - 2T(x_j, y_k, t_n)\} \\ &+\frac{D_a\tau}{h_y^2}\{T(x_j, y_k+h, t_n) \\ &+T(x_j, y_k-h, t_n) - 2T(x_j, y_k, t_n)\} \quad (3) \end{aligned}$$

where

$$\begin{aligned} x_{k+1} - x_k &= h_x \\ y_{j+1} - y_j &= h_y \\ t_{n+1} - t_n &= \tau_{int}. \quad (4) \end{aligned}$$

Using these equations, we calculated the time response of the current on the side of the QW to the input step current on the edge of the cladding layer at the p-side OCL, and the

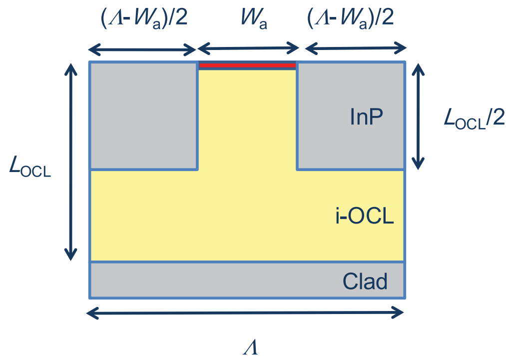

Fig. 3. Model used in the calculation.

TABLE I
PARAMETERS USED IN THE CALCULATION

Time interval	τ_{int}	5×10^{-16} s
x spacing	h_x	2 nm
y spacing	h_y	2 nm
Hole mobility	μ_h	100 cm^2/V/s
Diffusion coefficient	$D_h = k_B T/q\ \mu_h$	2.6 cm^2/s
Pitch	Λ	240 nm

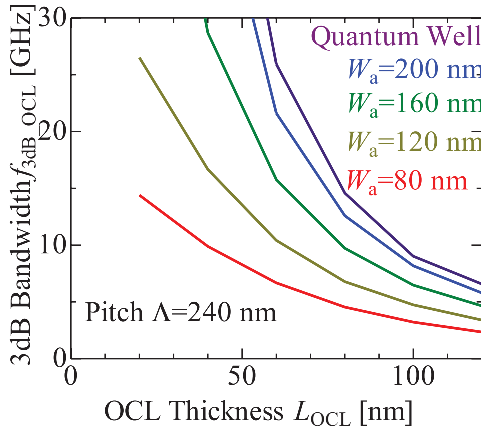

Fig. 4. 3-dB bandwidth dependence on various wire widths.

3 dB frequency f_{3dB_OCL}, which is limited by the diffusion time depending on the thickness of the OCL (L_{OCL}) and the width of the wirelike active region (W_a), was estimated from the rise time t_{rise} using an approximation of $f_{3dB_OCL} \sim 0.35/t_{rise}$. Figure 3 shows the model used for the calculation, and parameters used are listed in Table 1. The pitch Λ is 240 nm and the thickness of the embedded InP layer in the groove region is assumed to be half of L_{OCL}. The typical value of 100 cm^2/V/s was used for the mobility of holes.

Figure 4 shows the calculated f_{3dB_OCL} dependence on the OCL thickness for various widths of the wirelike active region. It is seen that $f_{3dB_OCL,QW}$ for lasers consisting of a QW active region is inversely proportional to the square of L_{OCL}, and it is approximately 9.5 GHz in the case of $L_{OCL} = 100$ nm, while that for DFB/DR lasers consisting of wirelike active regions $f_{3dB_OCL,Wirelike}$ is approximately 3 GHz in the case of $L_{OCL} = 100$ nm. f_{3dB_OCL} reduces as the width of the active region becomes narrower, and $f_{3dB_OCL,Wirelike}$ becomes less than $(W_S/\Lambda) f_{3dB}$ because carriers injected into the OCL beneath the central part of the groove region should be transported an additional distance of $\Lambda/2$ compared with those injected into the OCL beneath the wirelike active regions.

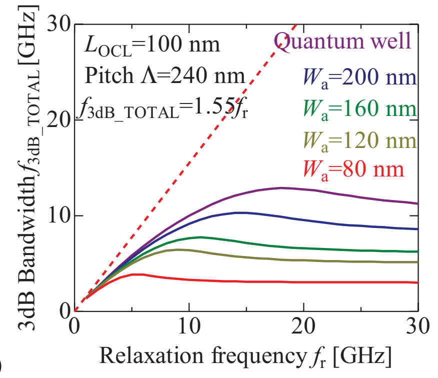

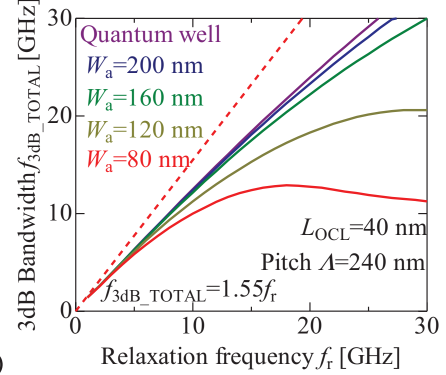

Fig. 5. Relationship between f_r and $f_{3\ dB_TOTAL}$ on various wire widths. (a) 100 nm of L_{OCL}. (b) 40 nm of L_{OCL}. Dashed lines denote the relation of $f_{3\ dB_TOTAL} = 1.55\ f_r$ (showing photon life time limit).

Next, the relationship between the f_r and total 3dB bandwidth $f_{3dB\ TOTAL}$ was calculated by solving the frequency response, Eq. (5) [19], and is shown in Figs 5(a) and 5(b) for $L_{OCL} = 100$ nm and 40 nm, respectively. It is noteworthy that the f_{3dB_TOTAL} tends to saturate for $L_{OCL} = 100$ nm due to the limitation of carrier transport whereas such tendency is not so strong for $L_{OCL} = 40$ nm.

$$M(\omega) = \left(\frac{1}{1 + j\omega\tau_{OCL}}\right) \frac{A}{\omega_r^2 - \omega^2 + j\omega\gamma}. \qquad (5)$$

$f_{3dB,Wirelike} = 10$ GHz can be attained for $W_S = 80$ nm and $L_{OCL} = 40$ nm, but a thinner OCL results in less optical confinement in the active region. Therefore, introducing a thinner OCL with consideration of the balance of the optical confinement factor and carrier transport is important to achieve high-speed and low-power-consumption DR lasers with wirelike active regions.

III. DEVICE STRUCTURES AND FABRICATION PROCESS

Two kinds of DR lasers with a relatively thick (120 nm) and thin (40 nm) OCL beneath the active regions were fabricated

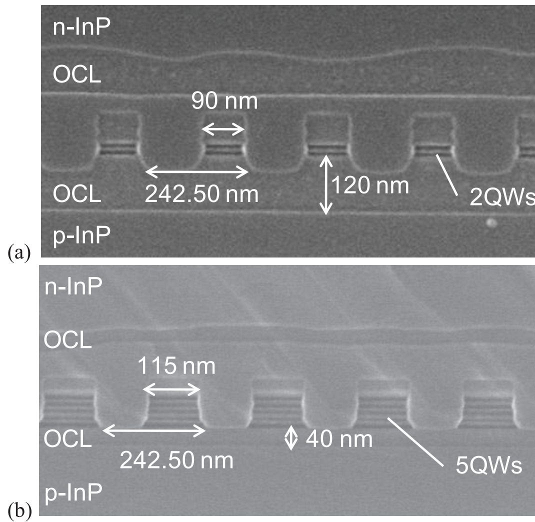

Fig. 6. Cross-sectional SEM views of the DFB section of (a) thick OCL device: a two-QW active region with OCL thickness of 120 nm and (b) thin OCL device: a five-QW active region with an OCL thickness of 40 nm.

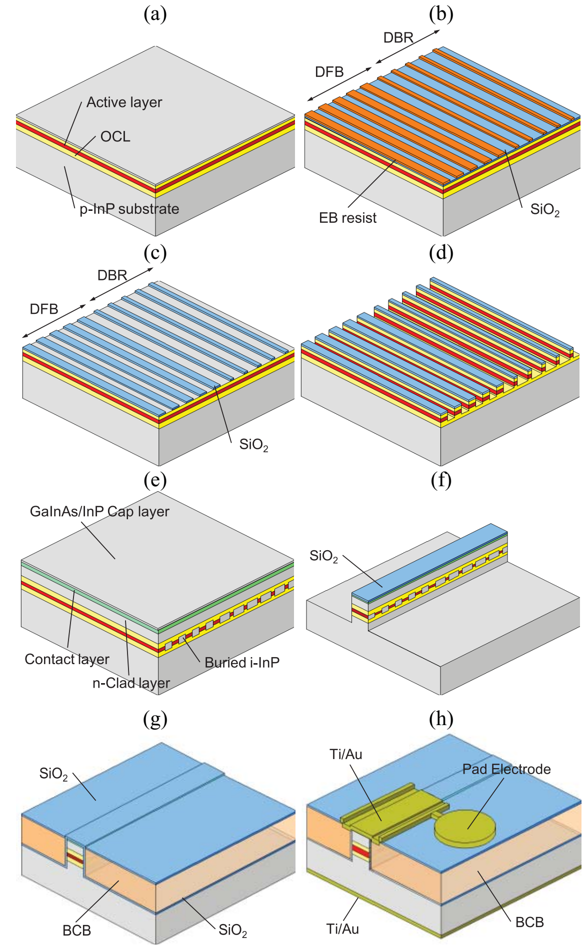

Fig. 7. Fabrication processes. (a) Initial wafer. (b) EB lithography. (c) CF_4 RIE. (d) CH_4/H_2 RIE. (e) Regrowth. (f) Stripe etching. (g) BCB coating. (h) Deposition Electrodes.

and their lasing properties compared. Figure 6 shows cross-sectional scanning electron microscope views of (a) *the thick OCL device*: a double quantum-well (two-QW) wirelike active regions (W_a = 90 nm, Λ = 242.50 nm) with p-side OCL thickness of 120 nm and (b) *the thin OCL device*: five-QW wirelike active regions (W_a = 115 nm, Λ = 242.50 nm) with p-side OCL thickness of 40 nm. The optical confinement factor of the initial two QWs is 2.2% (1.1%/well), while that of the five QWs is 4.75% (0.95%/well). It is noted that although the thicknesses of the n-side OCL of the two structures differ, the difference has practically no effect owing to the much greater mobility of electrons. For example, using the typical electron mobility of InP as 5000 cm^2/v/s, the diffusion coefficient becomes 0.013 m^2/s. In such a case, the expected bandwidth results in $f_{3dB_OCL} > 40$ GHz with L_{OCL} of 300 nm, and hence the i-InP grown on the wirelike active regions can't be a limiting factor of the modulation bandwidth.

Figure 7 shows the fabrication processes for DR lasers with wirelike active regions using electron beam lithography (EBL), CH_4/H_2 reactive-ion-etching (RIE), and embedding growth by organometallic vapor-phase-epitaxy [16, 17]. EBL was carried out to produce the desired wirelike patterns, which were transferred to a SiO_2 mask to etch away the QWs and OCLs through CH_4/H_2 RIE. Undoped-InP was then regrown into the groove regions at 600 °C with a low growth speed, and an upper OCL (40 nm thick), an n-InP cladding layer, and a 50-nm-thick n^+-GaInAs contact layer were grown at 650 °C. Afterward, a high-mesa stripe structure was produced through a combination of wet chemical etching and CH_4/H_2 RIE. Benzocyclobutene was spin-coated and then etched back by CF_4/O_2 RIE to planarize the entire surface. Next, 50-nm-thick SiO_2 was deposited and contact windows were opened. Finally, the substrate side was polished to a wafer thickness of around 100–150 μm, and Ti/Au was evaporated onto the p- and n-sides and lift-off was carried out for the contact pad on the n-side. An electrode pad of 80 μm diameter was produced so as to obtain a low parasitic constant for high modulation bandwidth.

IV. Lasing Characteristics and Discussion

Static and dynamic lasing characteristics of the fabricated DR lasers were measured after mounting the lasers on an AlN submount with a 50 Ω matching co-planar circuit with a series resistance of 40 Ω for impedance matching.

Figure 8 shows the current–light output (I–L) characteristic of the fabricated thick OCL device with two-QW wirelike active regions and L_{OCL} = 120 nm. Both facets were simply cleaved and no facet coating was applied. Under room-temperature continuous-wave (RT-CW) conditions, a low threshold current (I_{th}) of 1.0 mA and differential quantum efficiency from the front facet (η_{df}) of 19% were obtained with a DFB section length of 170 μm and stripe width of 2.0 μm. The threshold current density normalized by the area of the contact window (170 μm × 2.0 μm) was 294 A/cm^2, which was around 3 times the record low value (94 A/cm^2) of the DFB laser with two-QW wirelike active regions with a relatively long cavity (600 μm) and wide mesa stripe (19.5 μm) structure [21]. The lowest threshold current of 0.7 mA was reported for the DFB laser with two-

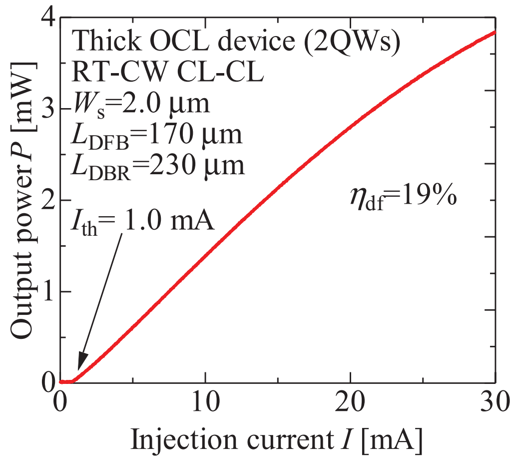

Fig. 8. Injection current–light output power ($I - L$) characteristic of thick OCL device.

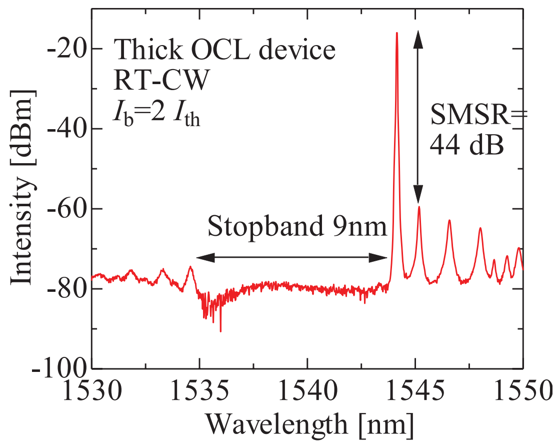

Fig. 9. Lasing spectrum of the thick OCL device.

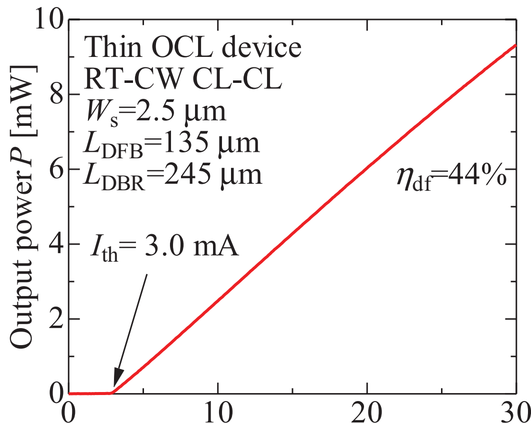

Fig. 10. Injection current–light output power ($I - L$) characteristic of the thin OCL device.

QW wirelike active regions with buried hetero (BH) structure and a similar cavity length (200 μm) and a stripe width of 2.3 μm [22, 23], and the threshold current density was 130–140 A/cm^2. Since the surface recombination velocity of the injected carriers at the regrown interfaces of the BH structure is very low compared with that of the sidewalls

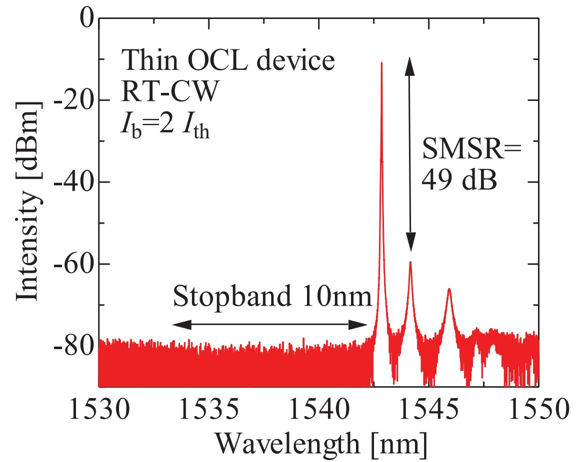

Fig. 11. Lasing spectrum of the thin OCL device.

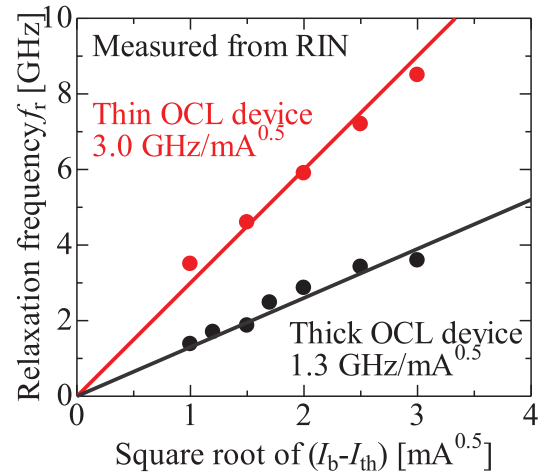

Fig. 12. Relaxation frequencies of DR lasers from RIN measurement.

of the high mesa stripe geometry, slightly higher threshold current density of the present DR laser can be attributed to non-radiative carrier recombinations at the sidewalls.

Figure 9 shows the lasing spectrum under an RT-CW condition with a bias current of $2I_{th}$, where single-mode operation was obtained with an SMSR of 44 dB, and a wide stopband width of 9 nm, which well agrees with the calculated index-coupling coefficient of 360 cm^{-1}, was confirmed.

Figure 10 shows the current–light output (I–L) characteristic of the thin OCL device with five-QW wirelike active regions and L_{OCL} = 40 nm. Again, both facets were simply cleaved and no facet coating was applied. Under an RT-CW condition, a threshold current (I_{th}) of 3.0 mA and high differential quantum efficiency from the front facet (η_{df}) of 44% were obtained with a DFB section length of 135 μm and stripe width of 2.5 μm. The threshold current density normalized by the area of the contact window (135 μm × 2.5 μm) was 889 A/cm^2. Since the number of QWs was increased from 2 to 5 for high-speed modulation, the threshold current was 3 times that in Fig. 8 and our previous report [17].

Figure 11 shows the lasing spectrum under an RT-CW condition at a bias current of $2I_{th}$, where single-mode

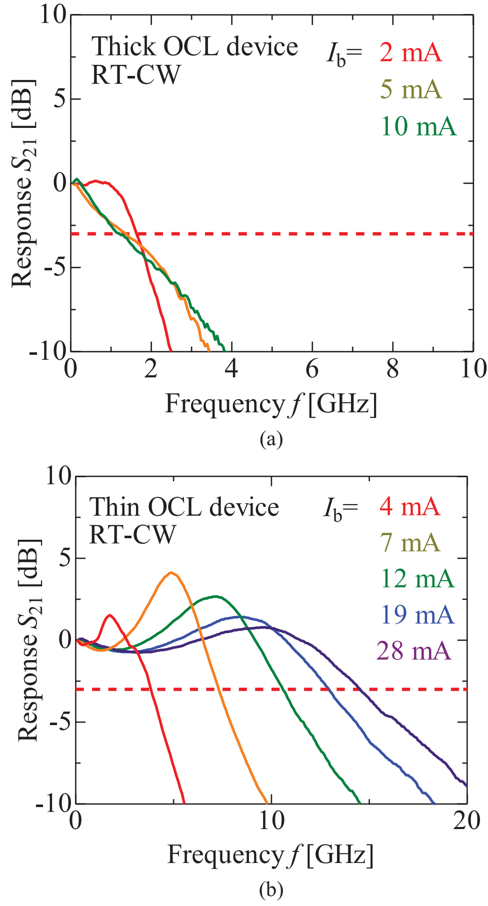

Fig. 13. (a) Thick OCL device. (b) Thin OCL device. Small-signal response of DR lasers.

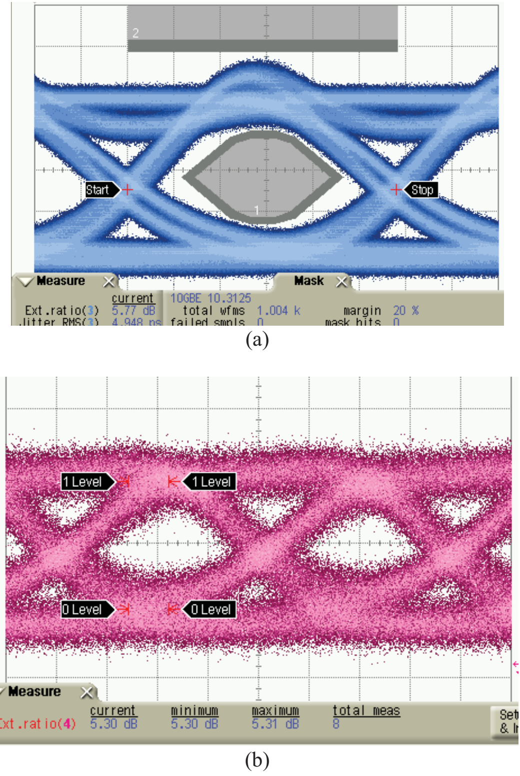

Fig. 14. Eye diagrams under high-speed modulation. (a) 10 Gb/s, $I = 10$ mA, and $V_{pp} = 0.53$ V. (b) 25 Gb/s, $I = 30$ mA, and $V_{pp} = 2.3$ V.

operation was obtained with an SMSR of 49 dB. Although the stopband was not clearly observed, the index-coupling coefficient of the grating was estimated from the cross sectional structure to be approximately 400 cm^{-1}, which corresponds to a stopband width of 10 nm.

Dynamic characteristics were measured from the relative intensity noise and the small-signal modulation response. Figure 12 shows the relaxation oscillation frequency f_r dependence on the square root of the bias current above the threshold $(I - I_{th})^{1/2}$, where f_r was measured from the peak frequency of the intensity-noise spectrum [24] to avoid the effect of the resistance–capacitance roll-off. The gradients of the plots were about 1.3 and 3.0 GHz/$mA^{1/2}$ for the thick and thin devices, respectively. The latter value is very high among those reported for GaInAsP materials and is comparable to that of state-of-art AlGaInAs QW lasers [5].

The small-signal modulation response was measured for various bias currents. Figure 13(a) shows the results for a thick-OCL device with $L_{OCL} = 120$ nm, where the 3 dB cut-off frequency (f_{3dB}) was limited to around 2 GHz even though the injection current was increased to 10 times the threshold. It is believed that the following three points are major causes of limiting direct modulation bandwidth of semiconductor lasers, i.e. relaxation oscillation frequency f_r,, parasitic RC, and carrier transport effect. As can be seen in Fig. 12, f_r of the thick OCL device was around 4 GHz at a bias current of $I_b = 10$mA, hence the corresponding f_{3dB} should be around 1.55 $f_r = 6$ GHz if there is no other restrictions. But observed f_{3dB} was only 2 GHz. Since f_{3dB} of over 15 GHz.was obtained for the thin OCL device having the same mesa-stripe geometry and the same electrode pad size with those of the thick OCL device, parasitic RC can't be the reason for poor modulation bandwidth of the DR laser with thick OCL. This measured bandwidth well agrees with that estimated for $L_{OCL} = 120$ nm and the wirelike active region width of 80 nm as shown in Fig. 4. On the other hand, in the thin-OCL device with $L_{OCL} = 40$ nm, f_{3dB} increased with bias current and reached 15 GHz at bias current of 28 mA. Since these small-signal modulation characteristics agree rather well with the calculated results shown in Fig. 4, the 3 dB bandwidth exceeding 20 GHz can be obtained by reducing the OCL thickness to 30 nm from the view point of carrier transport. However, we believe that it is possible to realize higher modulation speed by adopting a higher doping concentration in OCLs or an asymmetric layer structure of the p and n OCLs to shorten the transport time of holes without sacrificing the optical confinement factor in the active region. For high-speed direct modulations, further investigations on the optimal structure of the DR lasers with wirelike active regions are important.

Finally, we carried out large-signal direct modulation experiments at 10 and 25 Gbps with $2^{31} - 1$ pseudorandom bit sequence data streams for non-return-to-zero signals. As seen in Fig. 14(a), a very clear eye opening was obtained for 10 GbE mask test of 20% margin with bias current of only 10 mA and modulation voltage of 0.53 V_{pp}. Figure 14(b)

shows the eye diagram for 25 Gbps modulation, where the bias current was kept at 30 mA. In comparison with 10 Gps modulation, a clear eye opening was not obtained and a peak-to-peak modulation voltage of 2.3 V_{pp} was required to obtain an extinction ration of about 5 dB.

V. Conclusion

We revealed that carrier transport is a dominant limiting factor of the direct modulation speed of DFB and DR lasers with wirelike active regions and experimentally confirmed this finding using direct modulation characteristics of two DR lasers with different layer structures. A theoretical calculation showed that the carrier transport time in the OCL beneath the embedded InP layer strongly affects the modulation bandwidth, and indicates the necessity of thinner OCL design. By adopting thin OCLs of 40 nm and five quantum wells for higher modulation speed, the slope of the relaxation oscillation frequency f_r of 3.0 GHz/mA$^{0.5}$ was obtained owing to the low-threshold current characteristics of DR lasers, and 3 dB bandwidth over 15 GHz was achieved with relatively low bias current of 28 mA. Furthermore, a mask test of 10 GbE with 20% margin was passed with bias current as low as 10 mA and modulation voltage of 0.53 V_{p-p}. These results show that the DR laser with wirelike active regions is promising as a light source for access network applications and optical interconnections.

Acknowledgment

The authors would like to thank M. Asada, F. Koyama, T. Mizumoto, and Y. Miyamoto of the Tokyo Institute of Technology, Tokyo, Japan, for fruitful discussions. S. Lee and M. Shirao acknowledge the Japan Society for Promotion of Science for research fellowships for young scientists.

References

[1] A. Garreau, M.-C. Cuisin, J.-G. Provost, F. Jorge, A. Konczykowska, C. Jany, J. Decobert, O. Drisse, F. Blache, D. Carpentier, E. Derouin, F. Martin, N. Lagay, J. Landreau, and C. Kazmierski, "Wide temperature range operation at 43 Gbit/s of 1.55 μm InGaAlAs electroabsorption modulated laser with single active layer," in *Proc. 19th Indium Phosphide Rel. Mater. Conf.*, Matsue, Japan, May 2007, no. WeB1-2, pp. 358–360.

[2] T. Uesugi, N. Okada, T. Saito, T. Yamatoya, Y. Morita, and A. Sugitatsu, "1.3 μm EML TOSA for serial 40 Gb/s ethernet solution," in *Proc. Opt. Fiber Commun. Conf.*, San Diego, CA, Mar. 2010, no. OThC2, pp. 1–3.

[3] T. Yagisawa and T. Ikeuchi, "Compact 40-Gb/s EML module using broadband FPC connection technique," in *Proc. Opt. Fiber Commun. Conf.*, San Diego, CA, May 2010, no. OThC3, pp. 1–3.

[4] K. Sato, S. Kuwahara, Y. Miyamoto, and N. Shimizu, "40 Gbit/s direct modulation of distributed feedback laser for very-short-reach optical links," *Electron. Lett.*, vol. 38, no. 15, pp. 816–817, Jul. 2002.

[5] K. Nakahara, T. Tsuchiya, T. Kitatani, K. Shinoda, T. Taniguchi, T. Kikawa, M. Aoki, and M. Mukaikubo, "40-Gb/s direct modulation with high extinction ratio operation of 1.3-μm InGaAlAs multiquantum well ridge waveguide distributed feedback lasers," *IEEE Photon. Technol. Lett.*, vol. 19, no. 19, pp. 1436–1438, Oct. 2007.

[6] K. Otsubo, M. Matsuda, K. Takada, S. Okumura, M. Ekawa, H. Tanaka, S. Ide, K. Mori, and T. Yamamoto, "1.3-μm AlGaInAs multiple-quantum-well semi-insulating buried-heterostructure distributed-feedback lasers for high-speed direct modulation," *IEEE J. Sel. Topics Quantum Electron.*, vol. 5, no. 3, pp. 687–694, May–Jun. 2009.

[7] K. Adachi, K. Shinoda, T. Kitatani, Y. Matsuoka, T. Sugawara, and S. Tsuji, "Wide temperature range 25 Gb/s direct modulation of 1.3-μm lens-integrated surface emitting laser," in *Proc. IEICE Soc. Meet.*, Sep. 2010, no. C-4-1, p. 191.

[8] M. Radziunas, A. Glitzky, U. Bandelow, M. Wolfrum, U. Troppenz, J. Kreissl, and W. Rehbein, "Improving the modulation bandwidth in semiconductor lasers by passive feedback," *IEEE J. Sel. Topics Quantum Electron.*, vol. 13, no. 1, pp. 136–142, Jan.–Feb. 2007.

[9] U. Troppenz, J. Kreissl, W. Rehbein, C. Bornholdt, B. Sartorius, and M. Schell, "40 Gbit/s directly modulated passive feedback laser," in *Proc. 20th Int. Conf. Indium Phosphide Rel. Mater.*, May 2008, pp. 1–4.

[10] O. Kjebon, M. N. Akram, and R. Schatz, "40 Gb/s transmission experiment using directly modulated 1.55 μm DFB lasers," in *Proc. 15th Indium Phosphide Rel. Mater. Conf.*, Santa Barbara, CA, May 2003, no. FA1.2, pp. 495–498.

[11] G. P. Li, T. Makino, R. Moore, N. Puetz, K. W. Leong, and H. Lu, "Partly gain-coupled 1.55 μm strained-layer multiquantum-well DFB lasers," *IEEE J. Quantum Electron.*, vol. 29, no. 6, pp. 1736–1742, Jun. 1993.

[12] H. Lu, T. Makino, and G. P. Li, "Dynamic properties of partly gain-coupled 1.55-μm DFB lasers," *IEEE J. Quantum Electron.*, vol. 31, no. 8, pp. 1443–1450, Aug. 1995.

[13] N. Nunoya, M. Nakamura, M. Morshed, S. Tamura, and S. Arai, "High-performance 1.55-μm wavelength GaInAsP-InP distributed-feedback lasers with wirelike active regions," *IEEE J. Sel. Topics Quantum Electron.*, vol. 7, no. 2, pp. 249–258, Jun. 2001.

[14] J.-I. Shim, K. Komori, S. Arai, I. Arima, Y. Suematsu, and R. Somchai, "Lasing characteristics of 1.5 μm GaInAsP-InP SCH-BIG-DR lasers," *IEEE J. Quantum Electron.*, vol. 27, no. 6, pp. 1736–1745, Jun. 1991.

[15] K. Ohira, T. Murayama, H. Yagi, S. Tamura, and S. Arai, "Distributed reflector laser integrated with active and passive grating sections using lateral quantum confinement effect," *Jpn. J. Appl. Phys.*, vol. 42, no. 8A, pp. L921–L923, Aug. 2003.

[16] K. Ohira, T. Murayama, S. Tamura, and S. Arai, "Low-threshold and high-efficiency operation of distributed reflector lasers with width-modulated wirelike active regions," *IEEE J. Sel. Topics Quantum Electron.*, vol. 11, no. 5, pp. 1162–1168, Sep.–Oct. 2005.

[17] T. Shindo, S. Lee, D. Takahashi, N. Tajima, N. Nishiyama, and S. Arai, "Low-threshold and high-efficiency operation of distributed reflector laser with wirelike active regions," *IEEE Photon. Technol. Lett.*, vol. 21, no. 19, pp. 1414–1416, Oct. 2009.

[18] S. Lee, S. M. Ullah, T. Shindo, K. Davis, N. Nishiyama, and S. Arai, "Bit-error-rate measurement of GaInAsP/InP distributed reflector laser with wirelike active regions," in *Proc. 20th Int. Conf. Indium Phosphide Rel. Mater.*, Versaille, France, May 2008, no. MoA2-3, pp. 1–4.

[19] R. Nagarajan, M. Ishikawa, T. Fukushima, R. S. Geels, and J. E. Bowers, "High speed quantum-well lasers and carrier transport effects," *IEEE J. Quantum Electron.*, vol. 28, no. 10, pp. 1990–2008, Oct. 1992.

[20] R. Nagarajan, T. Fukushima, M. Ishikawa, J. E. Bowers, R. S. Geels, and L. A. Coldren, "Transport limits in high-speed quantum-well lasers: Experiment and theory," *IEEE Photon. Technol. Lett.*, vol. 4, no. 2, pp. 121–123, Feb. 1992.

[21] M. Nakamura, N. Nunoya, H. Yasumoto, M. Morshed, K. Fukuda, S. Tamura, and S. Arai, "Very low threshold current density operation of 1.5-μm DFB lasers with wire-like active regions," *Electron. Lett.*, vol. 36, no. 7, pp. 639–640, Mar. 2000.

[22] N. Nunoya, M. Nakamura, H. Yasumoto, M. Morshed, K. Fukuda, S. Tamura, and S. Arai, "Sub-milliampere operation of 1.55 μm wavelength high index-coupled buried heterostructure distributed feedback lasers," *Electron. Lett.*, vol. 36, no. 14, pp. 1213–1214, Jul. 2000.

[23] N. Nunoya, M. Nakamura, M. Morshed, S. Tamura, and S. Arai, "High-performance 1.55-μm wavelength GaInAsP-InP distributed-feedback lasers with wirelike active regions," *IEEE J. Sel. Topics Quantum Electron.*, vol. 7, no. 2, pp. 249–258, Feb. 2001.

[24] M. C. Tatham, I. F. Lealman, Colin P. Seltzer, L. D. Westbrook, and D. M. Cooper, "Resonance frequency, damping, and differential gain in 1.5 mm multiple quantum-well lasers," *IEEE J. Quantum Electron.*, vol. 28, no. 2, pp. 408–414, Feb. 1992.

Daisuke Takahashi (S'10–M'11) received the B.E. and M.E. degrees in electrical and electronic engineering from the Tokyo Institute of Technology, Tokyo, Japan, in 2009 and 2011, respectively.

SeungHun Lee (S'08–M'10) received the B.E., M.E., and Ph.D. degrees in electrical and electronic engineering from the Tokyo Institute of Technology, Tokyo, Japan, in 2006, 2008, and 2010, respectively.

He joined Samsung Electronics Co., Ltd., Seoul, Korea, in 2010.

Dr. Lee is a member of the IEEE Photonics Society.

Mizuki Shirao (S'08–M'11) received the B.E., M.E., and Ph.D. degrees in electrical and electric engineering from the Tokyo Institute of Technology, Tokyo, Japan, in 2007, 2009, and 2011, respectively.

He is a member of the Japan Society of Applied Physics.

Takahiko Shindo (S'10) received the B.E. and M.E. degrees in electrical and electronic engineering from the Tokyo Institute of Technology, Tokyo, Japan, in 2008 and 2010, respectively. He is currently pursuing the Ph.D. degree with the Quantum Electronics Research Center, Tokyo Institute of Technology.

He has been a Research Fellow with the Japan Society for the Promotion of Science, Tokyo, since 2010. His current research interests include photonic integrated devices on a silicon platform.

Mr. Shindo is a Student Member of the Japan Society of Applied Physics.

Keisuke Shinno received the B.E. degree in electrical and electronic engineering from the Tokyo Institute of Technology, Tokyo, Japan, in 2010. He is currently pursuing the M.E. degree with the same institution.

His current research interests include semiconductor lasers for photonic integration on a silicon platform.

Mr. Shinno is a Student Member of the Japan Society of Applied Physics.

Tomohiro Amemiya (S'06–M'09) received the B.S., M.S., and Ph.D. degrees in electronic engineering from the University of Tokyo, Tokyo, Japan, in 2004, 2006, and 2009, respectively.

He was with the Quantum Electronics Research Center, Tokyo Institute of Technology, Tokyo, in 2009, where he is currently an Assistant Professor. His current research interests include the physics of semiconductor light-controlling devices, metamaterials for optical frequency, magneto-optical devices, and processing technologies for fabricating these devices.

Dr. Amemiya is a member of the Optical Society of America, the American Physical Society, and the Japan Society of Applied Physics. He was the recipient of the IEEE Photonics Society Annual Student Paper Award in 2007 and the IEEE Photonics Society Graduate Student Fellowship in 2008.

Nobuhiko Nishiyama (M'01–SM'07) was born in Yamaguchi Prefecture, Japan, in 1974. He received the B.E., M.E., and Ph.D. degrees from the Tokyo Institute of Technology, Tokyo, Japan, in 1997, 1999, and 2001, respectively. During his Ph.D. work, he demonstrated single-mode 0.98 and 1.1 μm vertical cavity surface emitting laser (VCSEL) arrays with stable polarization using misoriented substrates for high-speed optical networks as well as metal–organic chemical vapor deposition-grown GaInNAs VCSELs.

He joined Corning Inc., Corning, NY, in 2001, and worked with the Semiconductor Technology Research Group. At Corning Inc., he worked on several subjects including short-wavelength lasers, 1060-nm DFB/DBR lasers, and long-wavelength InP-based VCSELs, demonstrating state-of-the-art results, such as 10-Gbit/s isolator-free and high-temperature operations of long-wavelength VCSELs. He has been an Associate Professor with the Tokyo Institute of Technology, since 2006. His current interests include laser transistors, silicon-photonics, III–V silicon hybrid optical devices, and THz-optical signal conversions involving optics-electronics-radio integration circuits.

Dr. Nishiyama received an Excellent Paper Award from the Institute of Electronics, Information and Communication Engineers of Japan in 2001 and the Young Scientists Prize in the Commendation for Science and Technology from the Minister of Education, Culture, Sports, Science and Technology in 2009. He is a member of the Japan Society of Applied Physics, the Electronics, Information and Communication Engineers, and the IEEE Photonics Society.

Shigehisa Arai (M'83–SM'06–F'10) was born in Kanagawa Prefecture, Japan, in 1953. He received the B.E., M.E., and D.E. degrees in electronics from the Tokyo Institute of Technology, Tokyo, Japan, in 1977, 1979, and 1982, respectively. During his Ph.D. work, he demonstrated room-temperature CW operations of 1.11–1.67 μm long-wavelength lasers fabricated by a liquid-phase-epitaxy as well as their single-mode operations under a rapid direct modulation.

He joined the Department of Physical Electronics, Tokyo Institute of Technology, as a Research Associate in 1982, and the AT&T Bell Laboratories, Holmdel, NJ, as a Visiting Researcher from 1983 to 1984, on leave from the Tokyo Institute of Technology. He then became a Lecturer in 1984, an Associate Professor in 1987, and a Professor with the Research Center for Quantum Effect Electronics and the Department of Electrical and Electronic Engineering in 1994. He has been a Professor with the Quantum Nanoelectronics Research Center, Tokyo Institute of Technology, since 2004. His current research interests include photonic integrated devices such as dynamic-single-mode and wavelength-tunable semiconductor lasers, semiconductor optical amplifiers, and optical switches/modulators, studies on low-damage and cost-effective processing technologies of ultrafine structures for high-performance lasers and photonic integrated circuits on silicon platforms.

Dr. Arai has been a member of the Optical Society of America, a fellow of the Japan Society of Applied Physics since 2008, the IEEE Photonics Society since 2010, and the Institute of Electronics, Information and Communication Engineers (IEICE) since 2011. He received an Excellent Paper Award from the IEICE of Japan in 1988, the Michael Lunn Memorial Award from the Indium Phosphide and Related Materials Conference in 2000, Prizes for Science and Technology including a Commendation for Science and Technology from the Minister of Education, Culture, Sports, Science and Technology in 2008, and an Electronics Society Award and an Achievement Award from IEICE in 2008 and 2011, respectively.